Fish and Shellfish Immunology 89 (2019) 710–718

Contents lists available at ScienceDirect

Fish and Shellfish Immunology

journal homepage: www.elsevier.com/locate/fsi

Full length article

Feed and immersion challenges with lymphocystis disease virus (LCDV) reveals specific mechanisms for horizontal transmission and immune response in senegalese sole post-larvae

Carlos Carballo[a], Juan B. Ortiz-Delgado[b], Concha Berbel[a], Dolores Castro[c], Juan J. Borrego[c], Carmen Sarasquete[b], Manuel Manchado[a,*]

[a] IFAPA Centro El Toruño, Junta de Andalucía, Camino Tiro Pichón s/n, 11500, El Puerto de Santa María, Cádiz, Spain
[b] Instituto de Ciencias Marinas de Andalucía-ICMAN, CSIC-Campus Universitario Río San Pedro, Puerto Real, 11510, Cádiz, Spain
[c] Universidad de Málaga, Departamento de Microbiología, Campus Teatinos, 29071, Málaga, Spain

ARTICLE INFO

Keywords:
LCDV
Horizontal transmission
Immune gene expression
Senegalese sole

ABSTRACT

The horizontal transmission of lymphocystis disease virus (LCDV) through contaminated water and feed (using artemia as vehicle) and the associated immune gene expression profiles in Senegalese sole post-larvae were investigated. All specimens analyzed were positive for LCDV DNA detection at 1-day post-challenge (1 dpc) with the highest viral levels in specimens infected through the immersion route. However, the percentage of LCDV-positive animals and number of viral DNA copies dropped progressively at 2 and 7 dpc. The histological analysis identified structural changes in the skin, muscle and gills of sole post-larvae LCDV-challenged by immersion. *In situ* hybridization confirmed a wide distribution of LCDV in the skin, gut, surrounding vessels in trunk muscle and head kidney in the immersion route, while the signals were restricted to the liver and *lamina propria* in the feeding treatment. Expression analysis using a set of 22 genes related to innate immune defense system demonstrated clear differences in the time-course response to LCDV as function of the infection route. Most antiviral defense genes, the proinflammatory cytokines, the complement c3, g-type lysozyme and T-cell markers *cd4* and *cd8a* were rapidly induced in the feeding-infected post-larvae, and they were remained activated at 2 dpc. In contrast, in the immersion-infected post-larvae the induction of most defensive genes was delayed, with a low intensity at 2 dpc. All these data demonstrate that LCDV can horizontally infect Senegalese sole post-larvae through the water or feed although with different patterns of histopathological disorders, virus distribution and route-specific expression profiles.

1. Introduction

The lymphocystis disease (LCD) is a viral pathology that affects more than one hundred fish species worldwide both in freshwater and marine environments (reviewed in Ref. [1]). The causative agent is the lymphocystis disease virus (LCDV) that belongs to the genus *Lymphocystivirus*, family *Iridoviridae*, and exhibits a marked tropism towards dermal fibroblasts. The typical lesions, known as lymphocysts, have a nodular aspect that in massive infections can spread and cover most of the skin body surface including fins [2]. In the Mediterranean basin and European South Atlantic coasts, LCDV infections are mainly identified in hatcheries producing gilthead seabream (*Sparus aurata*) appearing as self-limiting episodes with a high morbidity and low mortality, unless secondary infections or exacerbated cannibalism occur [3]. In most cases, the infected animals remain as asymptomatic carriers and only develop the disease under stress conditions. Experimental infections showed a long incubation time (~one month) before first detection of the characteristic lesions [1,4]. The integumentary lesions fully disappear in a few weeks, depending on the environmental temperature, and the recovered animals remain as asymptomatic carriers that convert the LCD in a chronic and recurrent problem in aquaculture hatcheries. Although LCDV has been detected in a wide range of fish species including the Senegalese sole (*Solea senegalensis*), the reported outbreaks of LCD in this species are still scarce [5,6].

The high rates of LCDV prevalence have been associated with both vertical and horizontal viral transmission [7]. Embryos from infected brooders were demonstrated to carry the LCDV on the egg surface [7]. However, the horizontal transmission by direct contact with infected

* Corresponding author. IFAPA Centro *El Toruño*Camino Tiro de Pichón s/n, 11500, El Puerto de Santa María (Cádiz), Spain.
E-mail address: manuel.manchado@juntadeandalucia.es (M. Manchado).

https://doi.org/10.1016/j.fsi.2019.04.049
Received 7 December 2018; Received in revised form 5 March 2019; Accepted 13 April 2019
Available online 15 April 2019
1050-4648/

animals or through contaminated water after breaking lymphocysts and the subsequent releasing of viral content has been hypothesized as the main mechanism that explains the high morbidity in highly susceptible species such as seabream, although no experimental evidences of waterborne viral transmission were still provided. Only the horizontal transmission through the supply of LCDV-infected live preys to the larvae during early developmental stages was demonstrated, representing an efficient way to deliver LCDV particles and to establish a systemic infection [7,8]. In Senegalese sole, there is no information about LCDV transmission routes. A previous study demonstrated that after intraperitoneal (i.p.) injection LCDV spreads rapidly through the bloodstream to invade several internal organs. The intense defensive response triggered in the host reduced progressively the number of viral particles but the LCDV could be detected 15 days after the experimental infection [9]. Although i.p. injection represents an adequate experimental approach to investigate the defensive mechanisms of fish against LCDV, further studies are necessary to establish the viral pathogenesis, the subsequent pathological alterations, and the defensive responses in the host.

Sole has been proposed as a model to study larval ontogeny, hormone regulation, epigenetic mechanisms or nutritional requirements in marine fish larvae due to its robustness to handling and the short larval rearing period [10]. Sole post-larvae (~20–30 days post-hatch) have a well-developed immune system highly responsive to environmental stimuli and pathogens [11–15]. This study aimed to determine the LCDV pathogenesis and defensive responses triggered in Senegalese sole post-larvae challenged using two transmission routes, by immersion in contaminated water or through feeding with LCDV-positive live artemia. Viral loads, tissue distribution and associated histopathological changes were determined. The time-course of the host defensive response was also analyzed using a panel of 22 immune genes. The data obtained provide new evidences of horizontal transmission for LCDV revealing significant differences in the histopathology, tissue distribution and host responses depending on the transmission route. The information generated is relevant to understand the mechanism of LCDV infection in marine fish and provide new clues for the control of this disease in aquaculture.

2. Material and methods

2.1. Virus collection, culture conditions

LCDV propagation in cell culture remains still a challenge, hence, LCDV genotype VII, the one that infect soles [6], was isolated from lymphocystis-diseased gilthead seabream specimens from a local farm (Southern Spain) as previously described in Carballo et al. [9]. Currently, LCDV outbreaks are quite uncommon in sole due its production in recirculation systems under strict biosafety measures. The virus infectious titer was calculated using the $TCID_{50}$ assay and validated by qPCR as previously described [5,16].

2.2. Experimental design

All procedures were authorized by the Bioethics and Animal Welfare Committee of IFAPA and given the registration number 10-06-2016-102 by the National authorities for regulation of animal care and experimentation.

Senegalese sole post-larvae (30 days post-hatch, dph) were supplied by Cupimar S.A. (San Fernando, Cadiz, Spain) and transported to IFAPA Centro El Toruño (El Puerto de Santa Maria, Cadiz, Spain). Post-larvae size was 7.9 ± 0.8 mm (n = 30) as determined by image analysis (Fiji 2.0.0). At arrival, the fish were distributed into 12 plastic trays (375 cm^2, 300 larvae per tray) containing 1l final volume of autoclaved seawater (salinity 35 g/l, 8 ppm oxygen). The trays were located in a temperature-controlled room and water temperature was maintained constant at 20 °C. Daily, water was manually renewed (~90%) and larvae were fed with artemia (~3000 metanauplii/tray). The animals were kept in these conditions for two days before starting the experiment. No mortality was registered in this period.

To carry out the immersion challenge, post-larvae from six trays were carefully transferred to 140 mm petri dishes containing 50 ml of sterile seawater. Three Petri dishes were added a LCDV suspension (10^5 $TCID_{50}$ ml^{-1} final concentration), whereas the remaining three plates received the same volume of phosphate buffer saline (PBS) and they were considered as the negative control group. After 2 h, post-larvae were collected using a 150 μm mesh, washed with sterile seawater and transferred back to the plastic trays. Thereafter, the animals were fed and handled as described above and disease signs monitored for 1 week. Post-larvae (n = 100) were sampled at 1, 2, and 7 days post-challenge (dpc). They were euthanized using overdose of tricaine methane sulfonate (MS-222), fixed in RNA-later (Invitrogen) and stored at −80 °C until use for viral detection and gene expression analysis. For histological analyses, larvae were fixed in PFA 4% as described in Refs. [17,18] and stored at −20 °C until use.

For the feed challenge, artemia metanauplii were enriched for 1 h using a LCDV suspension at 10^5 $TCID_{50}$/ml. Then, artemia were filtered, washed and resuspended in sterile seawater before supplying to the sole post-larvae. As indicated above, three plastic trays (n = 300) were used as negative controls and they were fed 3000 non-infected artemia (10 metanauplii/post-larva). The other three plastic trays were provided with the same quantity of LCDV-enriched live preys. After 1 h, no artemia was observed and the water was fully renewed using sterile seawater. The fish were maintained for 1 week and they were fed, sampled and monitored as indicated above for the immersion challenge.

2.3. Histological and in situ hybridization (ISH) analyses

Fixed samples were washed in PTW (1% PBS, 0.1% Tween 20) 3 times for 30 min each and then they were transferred to 10% EDTA/2% formaldehyde solution at 4 °C for 7 days. After fixation and decalcification, samples were washed 3 times in PTW as described above, embedded in paraffin and serially sectioned at 5–6 μm thickness as previously described [19]. The haematoxylin-eosin technique [20] was used for histological studies (n = 9–12 for each time and experimental group).

In order to detect the presence of viral DNA in larvae tissues, histological sections of non-infected (control) and infected post-larvae from immersion and oral challenges at 1, 2 and 7 dpc were analyzed by ISH (n = 3 for negative control and n = 6 for LCDV-infected soles at each sampling time) as previously described [21,22]. A fragment of the LCDV *mcp* gene was amplified using specific primers (RT-LCDV-F and RT-LCDV-R2) [23] and the following PCR program: 95 °C for 2 min, followed by 35 cycles of 1 min at 95 °C, 1 min at 53 °C and 10 min at 72 °C. The fragment was cloned into the TOPO-TA vector (Invitrogen) and the probe synthetized using the PCR DIG Probe Synthesis Kit (Roche). Dewased and rehydrated sections were permeabilised with Triton X-100, and then treated with proteinase-K (100 μg ml^{-1} in 0.1 M Tris buffer, pH 8) for 30 min at 37 °C. Target DNA in tissue sections and probe were simultaneously denatured at 95 °C for 5 min, and hybridization performed overnight at 55 °C. The slides were washed in saline sodium citrate buffer with 6 M urea and 0.2% (w/v) BSA for 10 min at hybridization temperature. Tissue sections were blocked with blocking reagent, and incubated with an anti-DIG monoclonal antibody (Roche Applied Science) conjugated to alkaline phosphatase for 1 h. The colorimetric detection of the hybridization signal was carried out with NBT/BCIP. Staining controls were performed in tissue sections by omitting the DNA probe.

2.4. Quantification of viral DNA

Three pools of artemia metanauplii (40 mg) were taken and analyzed after LCDV enrichment. In post-larvae, a total of n = 8 individuals

randomly sampled from triplicate trays at each time point (1, 2 and 7 dpc) were processed. Total DNA of artemia and whole post-larvae was isolated using ISOLATE II Genomic DNA Kit (Bioline). DNA samples were treated with RNase A (Bioline) following the manufacture's protocol. DNA was quantified spectrophotometrically using the Nanodrop ND-8000. Absolute quantification of viral DNA copies was carried out according to the protocol specified by Valverde et al. [16] using a CFX96™ Real-Time System (Bio-Rad) in a 20 µl final volume containing 200 ng of DNA, 300 nM each of specific forward and reverse primers, and 10 µl of iQ™ SYBR® Green Supermix (Bio-Rad). The amplification protocol used was as follows: initial 7 min denaturation and enzyme activation at 95 °C, 40 cycles of 30 s at 95 °C and 1 min at 59 °C.

2.5. RNA isolation and gene expression analysis

To investigate the innate immune responses and due to the small size of post-larvae, the specimens were dissected to keep the anterior portion of the body containing the head and the abdominal cavity. The caudal region containing mainly skin and muscle was discarded. This procedure allowed the enrichment of samples in those internal organs in which the virus concentrate before spreading toward the target tissues (skin and fins) (see Fig. 4). The anterior portion of larvae (n = 3) were suspended in 1 ml of TRI-Reagent (Sigma-Aldrich) and homogenized in the Fast-prep FG120 instrument (Bio101) using Lysing Matrix D (Q-Bio-Gene) for 60 s at speed setting 6. The aqueous phase was transferred to a column of Isolate II RNA Mini Kit (Bioline) and total RNA was treated twice with DNase I for 30 min following the manufacture's protocols.

To determine *mcp* gene expression, cDNA synthesis and qPCR assays were carried out as described in Carballo et al. [9]. The reference gene used was 18S rRNA [24].

To quantify host gene expression after LCDV challenge, the cDNA synthesis was carried out using the i*Script*™ cDNA Synthesis Kit (Bio-Rad) and the qPCR assays were carried out on a CFX96™ Real-Time System (Bio-Rad) using a 10-µl volume containing cDNA generated from 200 ng of original RNA template, 300 nM each of specific forward and reverse primers, and 5 µl of SYBR Premix Ex Taq (Takara, Clontech). Most of the primers were published elsewhere and they were sole-specific: *il1b, tnfa, clec, cxc10, ifn1, irf7, irf8, irf9* [25], *irf1, irf3* [9], *hsp90a* [26], *lysg* [11], *mx* [27] and *c3* [10]. Primers for *irf2, irf4, irf5, irf10, ifna3, cox2 cd4 and cd8a* were designed in this study (Table 1). The amplification protocol used was as follows: initial 7 min denaturation and enzyme activation at 95 °C, 40 cycles of 30 s at 95 °C, 15 s at 68 °C and 30 s at 72 °C. Each PCR assay was done in duplicate. The ubiquitin (*ub52*), hypoxanthine phosphoribosyltransferase (*hprt1*), and glyceraldehyde-3-phosphate dehydrogenase (*gapdh2*) genes were used as reference genes, and the sample from control group at 1 dpc was used as calibrator [24,28]. Relative mRNA expression was determined using the comparative method $2^{-(\Delta\Delta Ct)}$. Clustering analysis was carried out by PermutMatrix [29] using log2 transformation of fold-change with parameters set as following: Dissimilarity: Euclidean distance, Hierarchical: Complete Linkage Method, Seriation: Multiple-fragment heuristic (MF).

2.6. Statistical analysis

The qPCR data were log-transformed in order to comply with normality and homogeneity of variance. A two-way ANOVA was used to test the changes in gene expression after the viral challenge using treatments and time as fixed factors. When a significant effect of virus was determined, single ANOVAs were carried out. Statistical analyses were performed using SPSS v21 software (IBM).

3. Results

3.1. Quantification of viral DNA in LCDV-infected post-larvae

To demonstrate the horizontal transmission of LCDV in Senegalese sole post-larvae (30 dph), two different infection routes were assayed: water immersion (10^5 $TCID_{50}$/ml final concentration) and through feeding using artemia metanauplii. The viral concentration in the enrichment medium for artemia was the same used in the immersion challenge, and resulted in a viral load of (9.7 ± 1.4) x10^6 viral DNA copies/metanauplii. As expected in LCDV challenges, no mortality or signs of disease were observed during the trial (7 days).

Viral DNA was detected in 100% of LCDV-infected post-larvae at 1 dpc. The infection percentage dropped to 75.0–87.5% at 2 dpc and 62.5% at 7 dpc. Post-larvae from the non-infected control groups were PCR-negative at all time points analyzed.

The absolute quantification of viral DNA showed a higher viral load in immersion-infected post-larvae at 1 dpc (371 ± 150 viral DNA copies µg total DNA^{-1}) than at 2 and 7 dpc (47 ± 7 and 51 ± 5 viral DNA copies µg total DNA^{-1}, respectively) (Fig. 1). In contrast, the number of DNA copies remained low and constant in feeding-infected post-larvae (66 ± 9, 38 ± 5 and 40 ± 4 viral DNA copies µg total DNA^{-1} at 1, 2 and 7 dpc, respectively). No expression of *mcp* was detected through the trial.

3.2. Histological analysis

To identify specific lesions associated with the LCDV infection route, a comparative histological analysis between negative controls and infected fish was carried out. Histological sections of Senegalese sole post-larvae challenged by immersion at 2 dpc (Fig. 2A–H) showed

Table 1
Primers designed in this study. Target gene, amplicon size and unigene code in SoleaDB [9] are indicated.

Target	Primer	Sequence (5'→3')	Amplicon (bp)	Code
irf2	F	GCTCCTCCCACTCGTACCCGCTCCA	120	unigene45267
	R	TGTAGTTCCGCCTCCAGCCTGCACCAAC		
irf4	F	CCATCACTTTTCCGTTCCCGTACCCCGAG	102	unigene135376
	R	CGTCCGGCATCATCCACAAACGCACCC		
irf5	F	CGACCCTGCGAAGTGGAAAGCGAACCT	96	unigene37530
	R	TGCACCGGCGTCTCTTTGGTTCCGT		
irf10	F	AAGCCATGAACTGCCTGTTGTGTCACCTCG	119	unigene282743
	R	GGCCATCGGACCGCTCCAGTACACCC		
ifna3	F	ACTTGACTCATCGCTTCCTGATCGACACCA	84	unigene48491
	R	TGTCTGCTTGCTTCTGCATCGACACACAGG		
cox2	F	GTTTATCCCGGACCCGCAGGGCACCA	112	unigene535312
	R	AGCCGCGGTGAATGCAGGTCCTTTCT		
cd4	F	ACATCTATGCCCGTCACCATCCCCTGC	119	unigene10638_split_1
	R	ACGCCTGAAGACTGCCGAGGGAAGAATTGC		
cd8a	F	CCCAGACGAAGCCCCCCACGACCAC	105	unigene59609
	R	CCGGGCCCAGAATGAGCGGAGAGCA		

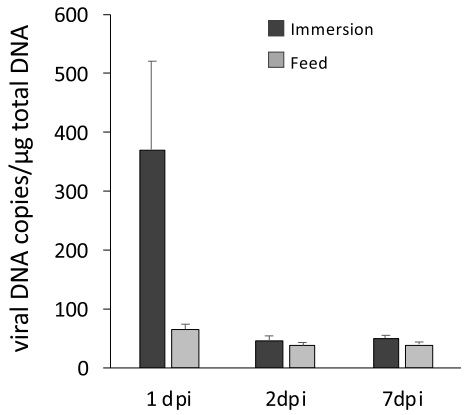

Fig. 1. LCDV DNA quantification in infected Senegalese sole post-larvae at 1, 2 and 7 dpc. Dark bars, water immersion challenge; light bars, feed (artemia metanauplii) challenge. Data were expressed as mean ± SEM.

hypertrophied epidermal mucous cells in the skin (100% specimens analyzed; Table 2) and a moderate shrinkage of muscular fibers from myotomes and a disorganization of collagen myosepts (92% fish) (Fig. 2B). In the gills, a moderate hyperplasia of interlamellar epithelium (78% fish) conducting to a lamellar obliteration and fusion of adjacent lamellae and the disorganization of gill filaments (67% fish) were found (Fig. 2D). At 7 dpc, the number of fish with histological changes in the skin was lower but all LCDV-infected soles had severe lamellar fusions in the gills (Fig. 2E) not observable in the controls (Fig. 2F and Table 2). No signs of histopathological disorders were detected in the gut, neither in the mucosa, the *lamina propria* or the muscle layers (Fig. 2G and H). In the post-larvae infected through feeding (Fig. 2I-L), mucous cells appeared hypertrophied in the anterior intestine at 2 dpc (92% specimens; Fig. 2J). In contrast, at 7 dpc, just a moderate atrophy of the mucosa layer and an apparent size-reduction of mucous cells were observed (Fig. 2L and Table 2).

3.3. In situ hybridization of viral DNA

Tissue localization of viral DNA in infected post-larvae revealed a clear route-specific distribution pattern (Fig. 3). Viral genome was detected only at 1 dpc in both viral transmission routes. LCDV was mainly detected in epithelial cells of dorsal fin, buco-pharyngeal cavity and intestine, in Malpighi cells of the epidermic layer and around the mucous cells in the skin, surrounding vasculature in trunk muscle and in head kidney when post-larvae were infected by immersion (Fig. 3C–H). Nevertheless, post-larvae infected through feeding only showed positive hybridization signals in the hepatic parenchyma and the *lamina propria*, with no signal in the intestinal epithelium (Fig. 3I and J). All negative controls failed to show any positive signal for viral DNA hybridization.

3.4. Gene expression analysis

To evaluate the defensive response triggered by post-larvae in response to both types of LCDV challenge, a set of 22 transcripts were analyzed comprising antiviral defenses [antiviral Mx protein, interferon 1 (*ifn1*), *ifna3* and nine interferon-related factors (IRFs) (*irf1*, *irf2*, *irf3*, *irf4*, *irf5*, *irf7*, *irf8*, *irf9*, *irf10*)], interleukin 1b (*il1b*), chemokines *tnfa* and *cxc10*, complement factor *c3*, PAMP receptor *clec*, the antigen differentiation *cd4* and *cd8a*, g-type lysozyme (*lysg*), the cyclooxygenase *cox2* and heat shock protein *hsp90aa*.

The clustering analysis clearly separated negative controls from LCDV-infected groups (Fig. 4, blue vs red and yellow squares) although with time- and infection route-specific branches. The LCDV-feeding infected group had the most intense and well-differentiated response at

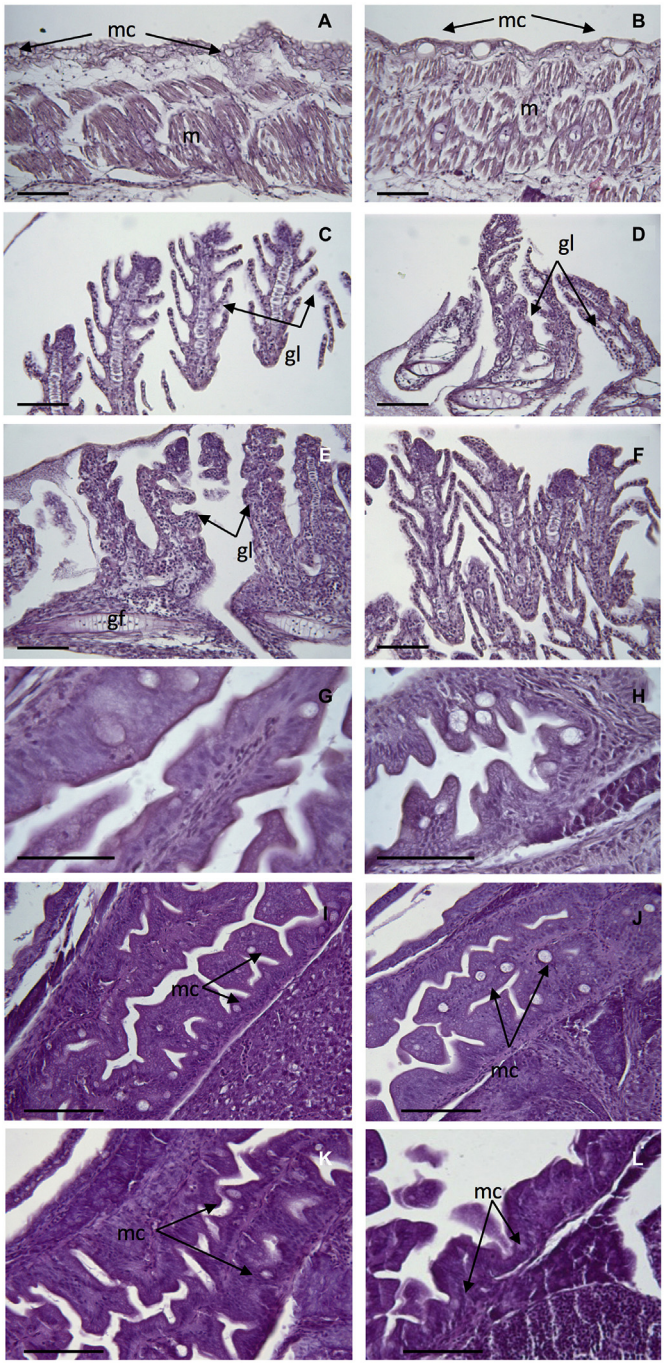

Fig. 2. Histopathology of LCDV infection in sole post-larvae. Immersion challenge: **(A)** Transversal section of the skin layer and subjacent musculature in one specimen from the negative control group. Note muscle fibers packed in blocks (myotomes) between sheets of collagen (myosepts); **(B)** epidermal mucous cells hypertrophy, shrinkage of muscular fibers and myosept disorganization in LCDV-infected sole; **(C,F)** histological sections of gills in negative controls; **(D)** moderate hyperplasia of interlamellar epithelium and lamellar obliteration and fusion in LCDV-infected sole at 2 dpc; **(E)** severe lamellar fusion in gills in LCDV-infected sole at 7 dpc; longitudinal sections of intestine from LCDV-infected **(G)** and negative control **(H)** post-larvae at 7 dpc. No signs of pathological disorders were detected. Feed challenge: **(I)** transversal section of anterior intestine in negative control at 2 dpc; **(J)** mucous cell hypertrophy in LCDV-infected sole at 2 dpc; transversal section of anterior intestine in negative control **(K)** and LCDV-infected **(L)** post-larvae at 7 dpc. Note a moderate atrophy of mucosa layer and an apparent size-reduction of mucous cells in infected specimens **(I)**. Scale bars represent 50 µm. gf: gill filament; gl: gill lamellae; mc: mucous cells; m: trunk muscle.

Table 2
Histopathological findings in different organs/tissues of *S. senegalensis* post-larvae at 1, 2 and 7 days post-LCDV challenge by immersion or feeding. The control group refers to the negative controls of both experimental trials.

Tissue and alteration	%animals[a]/surface scale[b]								
	Control			Immersion			Feed		
	1dpi	2dpi	7dpi	1dpi	2dpi	7dpi	1dpi	2dpi	7dpi
Skin									
Epidermal mucous cells hypertrophy	8/0-1	0/0	11/0-1	11/0-1	100/3	45/1-2	11/0-1	8/0-1	0/0
Shrinkage of muscular fibers	0/0	0/0	0/0	11/0-1	92/3	89/3	0/0	0/0	0/0
Gills									
Hyperplasia of interlamellar epithelium	8/0-1	8/0-1	11/0-1	11/0-1	78/2	100/3	11/0-1	8/0-1	11/0-1
Fusion of secondary lamellae	0/0	0/0	0/0	11/0-1	67/2	100/3	0/0	0/0	0/0
Gut									
Hypertrophy of intestinal mucous cells	0/0	0/0	0/0	0/0	0/0	0/0	0/0	92/3	11/0-1
Atrophy of mucous layer	0/0	0/0	0/0	0/0	0/0	0/0	0/0	8/0-1	89/3

[a] Percentage of animals with histological disorders (n = 9–12).
[b] Surface scale: 0 = no alteration; 1 = weak histological alteration restricted to small areas in the organ affected; 2 = moderate alteration with approx. half of the organ affected; 3 = strong alteration with histological changes spread through the whole organ.

1 and 2 dpc. In contrast, post-larvae infected by immersion had a moderate up-regulation of these genes with main transcriptional responses later at 2 dpc.

A detailed gene-specific analysis is depicted in Table 3. Expression profiles in post-larvae exposed to LCDV by immersion indicated a fast and statistically significant induction of proinflammatory cytokines *il1b* and *tnfa, cxc10* and *irf7* at 1 dpc. However, most antiviral defense genes (*ifn1*, *ifna3*, *mx*, *irf3*, and *irf9*), the complement factor *c3*, clec, *cox2* and *hsp90aa* were activated later at 2 dpc. The *tnfa* and *irf 7* also remained activated at 2 dpc. When compared with post-larvae infected through feeding, most antiviral defense genes (*ifn1*, *ifna3*, *mx*, *irf4*, *irf7*, *irf9,* and *irf10*) were activated faster, including the proinflammatory cytokines *il1b* and *tnfa*, the complement *c3*, *lysg*, *cxc10* and T-cell markers *cd4* and *cd8a*. Most of them remained up-regulated at 2 dpc but also a statistically significant increase in *irf2*, *irf3*, *irf5 cox2*, and *hsp90aa* expression was observed.

4. Discussion

Understanding the transmission routes used by LCDV to infect fish is critical to establish control and prevention measures in aquaculture facilities. Previous studies in gilthead seabream demonstrated that both vertical and horizontal transmission routes (through the live preys) play a key role in LCDV epidemiology (reviewed in Refs. [1,7,8]). However, it is important to demonstrate if other horizontal transmission ways behind the LCD spreading exist as well as their main pathological consequences. This study demonstrates that LCDV invades and spreads to internal organs in Senegalese sole post-larvae both by immersion in contaminated water and through the feeding using LCDV-enriched artemia metanauplii to establish a non-productive infection during the experimental period (7 dpc). Moreover, our data indicate that the transmission route determines specific tissue distribution patterns, histopathological lesions and time-course response of defensive genes. Immersion challenge resulted in the highest viral load at the beginning of the trial, even though the percentage of LCDV-positive animals and the estimated number of viral DNA copies were kept at low levels at the end of the trial in both experimental infections. These results agree with the fast clearance of LCDV from peripheral blood and the reduction of viral DNA copies in internal organs as infection progresses from 1 to 2 to 5–7 days in intraperitoneally infected Senegalese sole juveniles. This reduction in viral load was accompanied by a delay of intracellular viral multiplication from 5 to 15 days post-injection [9]. In this study, we did not detect virus replication within the first week after the LCDV challenges that could be due to a different temporal framework required to set a productive infection modulated by the transmission route and the triggered immune response.

Histological analysis confirmed the integrity of the skin barrier in post-larvae from the negative control groups, as expected. However post-larvae infected by immersion showed significant structural changes in the skin, muscle and gills at 2 dpc that were even more evident at 7 dpc due to the inflammatory response triggered by LCDV. The hypertrophy of mucous cells in the skin and gut indicated that LCDV triggered a defensive response in the host by modulating mucus production. The increase of mucous cells and their sialic acid glycoproteic content were also reported in LCDV-infected *S. aurata* [30] and it seems to be a key mechanism that interferes viral receptor binding and bacterial invasion [31–33]. This hypothesis is supported by previous observations in carp in which the removal of the skin mucous layer and the induction of epidermal lesions appear to play a major role in herpesvirus infection [34]. It is noteworthy that gill lamellae were also highly affected by LCDV waterborne infection. Architecture of this tissue accompanied by severe inflammation is also affected by herpesvirus infection in carp [33]. These results demonstrate that a specific defensive response was activated in both LCDV horizontal transmission routes with the skin and gills as the main portals to LCDV entry in the waterborne infections.

The tissue remodeling observed in peripheral organs matches with the distribution of LCDV genome mainly in external mucosa (skin and gut) but also in the head kidney. The identification of LCDV-hybridization signal surrounding vasculature clearly points out the bloodstream as the main dissemination via for LCDV after immersion challenge. This mechanism agrees with Carballo et al. [9] that also detected a rapid spreading of LCDV from the peritoneal cavity through the bloodstream previous to the establishment of a systemic infection in sole juveniles. Unlike the immersion exposure, the vehiculation of LCDV through the feed confined the viral signal to the intestinal *lamina propria* and hepatic parenchyma indicating a tight restriction to virus dissemination. In seabream larvae infected by feeding on LCDV-positive live preys viral antigens and genomes were firstly located in the digestive tract [7] but were detected in the skin after 48 h. All these data support the horizontal transmission of LCDV in Senegalese sole through contaminated water and feed, although the former route leads to a wider virus spread and tissue damages presumably as a part of the defensive response.

Immune organs in Senegalese sole develop very early in the pelagic stage [35] and a wide set of innate immune genes are highly expressed in pre-metamorphosis larvae while adaptive genes seem to appear later after metamorphosis [11–13]. Our study demonstrates a highly coordinated response of interferon-related genes, chemokines, cytokines, lysozyme, complement and T-cell markers in response to LCDV

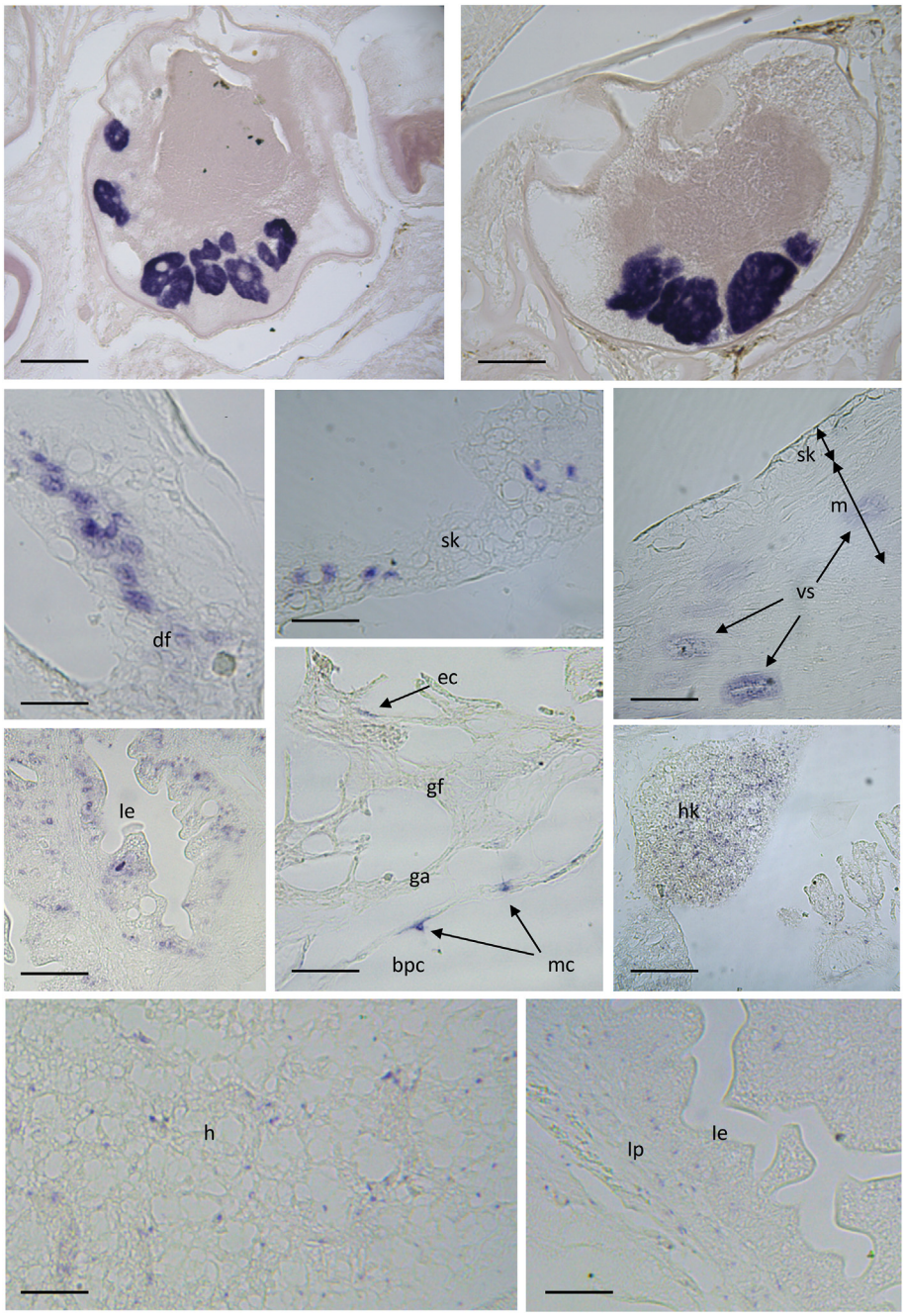

Fig. 3. Detection of LCDV by *in situ* hybridization. **(A)** and **(B)** Positive control of LCDV particles within lymphocysts in a naturally infected *S. aurata* specimen. In sole post-larvae infected by immersion at 1 dpc, hybridization signals (dark blue staining) can be observed in epithelial cells from dorsal fin **(C)**, Malpighi cells in the epidermic layer of the skin **(D)**, periphery of vasculature in trunk muscle **(E)**, epithelial cells from intestine **(F)**, mucous and epithelial cells from the buco-pharyngeal cavity **(G),** and in head kidney **(H)**. Post-larvae infected by feeding: hepatic parenchyma **(I)** and the *lamina propria*/submucosa **(J)**. Note absence of viral DNA in the intestinal epithelium. Scale bars represent 50 μm bpc: buco-pharyngeal cavity; df: dorsal fin; ec epithelial cells; gf: gill filament; ga: gill arch; h: hepatocytes; hk: head kidney; ie: intestinal epithelium; lp: *lamina propria*/submucosal layer; m: trunk muscle; mc mucous cells; sk: skin; vs: vascular system. (For interpretation of the references to color in this figure legend, the reader is referred to the Web version of this article.)

infection, confirming that young post-larvae (31 dph) were able to activate a specific defensive response although with temporal and intensity differences depending on the infection route. Delivery of viral particles through artemia triggered the faster and more intense response. This response was similar to that reported in LCDV-injected sole juveniles that display tissue-specific responses depending on the amount of viral DNA quantified in each tissue [9]. We hypothesize that the weaker and delayed expression response observed in the immersion-infected fish could be due to a low concentration of LCDV particles in water able to circumvent an intense immune response and reach blood vessels to disseminate throughout the organism. In contrast, artemia concentrated LCDV in the gut allowing a quick viral recognition and a potent and localized immune response that limit virus dissemination and pathogenesis. The observed differences in the triggered immune responses could be of interest for oral vaccination strategies and antigen delivery.

Expression profiles associated with LCD in gilthead seabream with pronounced lesions indicated a down-regulation of antiviral genes such as *ifn* and *irf3* and other involved in cellular immunity in the skin and head kidney of LCDV-positive fish [36]. In contrast, in flounder (*Paralichthys olivaceous*) LCDV triggers the expression of *irf2*, *irf3*, *irf5*, *irf7 irf8* and *irf9* in immune and non-immune organs [37–42] but down-regulates *isg15* and *mx* expression in the gills [42]. In Senegalese sole post-larvae, eight genes encoding different *irf* genes and *mx* were up-regulated, an expression profile similar to that found when LCDV was i.p. injected in sole juveniles [9]. The *in vitro* overexpression of *mx* from the gilthead seabream is essential to prevent the *in vitro* cytopathic effects of LCDV [43] and for the *in vivo* establishment of an antiviral state [27]. We hypothesized that the activation of the interferon pathway observed in this study could explain the progressive drop in LCDV copies and the lack of *mcp* expression in the period analyzed. It is also noteworthy the activation of an acute-phase inflammatory response

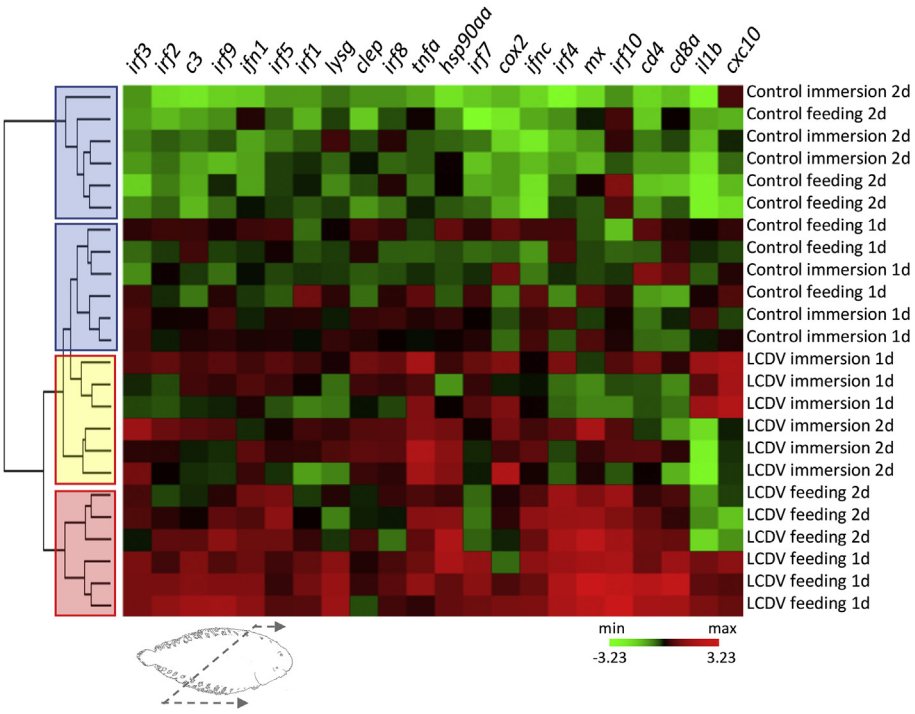

Fig. 4. Hierarchical clustering analysis based on differentially transcribed genes. Data were expressed as log2 of fold change. Green and red colors indicate low and high expression values according to the scale shown. The samples are identified on the right and included control and LCDV-infected post-larvae and transmission route (immersion or feed) at 1 and 2 dpc. The main clusters grouping the samples appear on the left [control (blue), infected by immersion (yellow) and feeding-infected (red)]. The cut section of Senegalese sole post-larva used for gene expression analysis is indicated below. (For interpretation of the references to color in this figure legend, the reader is referred to the Web version of this article.)

mediated by cytokines (*il1b* and *tnfa*), chemokines *cxc10* and cyclooxygenase *cox2* that increase vascular permeability and enhance the recruitment of inflammatory cells causing tissue remodeling and concertedly blocking LCDV replication [44,45]. Although some viruses use the chaperone Hsp90 for nucleic acid replication [46], the lack of *mcp* expression indicates that *hsp90* mRNA levels could be modulated to regulate cellular homeostasis after virus infection.

5. Conclusion

This study demonstrates that LCDV is horizontally transmitted to Senegalese sole post-larvae through both water and live preys. The virus shows a wider tissue distribution and higher viral loads when soles were challenged by immersion, with structural changes in skin and gills not observed in the feeding transmission route. The expression responses associated to LCDV infection revealed time and intensity differences indicating a clear activation of type I interferon system, proinflammatory cytokines and other molecules of innate immune system that plays a key role in the clearance of LCDV and tissue remodelling found in this study. All this information is relevant to understand the transmission routes of LCDV and will be useful to establish control measures in fish hatcheries.

Table 3
Gene expression fold changes (F-C) at 1 and 2 days after LCDV challenge by immersion or feeding. Two-way ANOVA for infection (i), time (t) and interaction (t*i) are indicated (*$P < 0.05$; **$P < 0.01$). When infection was significant, one-way ANOVA was carried out for each time (F-$C_{1\ or}$ F-C_2). Significance at $P < 0.05$ (*) is indicated. ns, not significant.

Gene name	Gene description	Immersion					Feed				
		F-C_1	F-C_2	i	t	t*i	F-C1	F-C_2	i	t	t*i
il1b	Interleukin 1β	2.4 ± 0.5*	0.8 ± 0.1	**	*	**	1.8 ± 0.1*	1.8 ± 0.3	*	**	**
tnfa	Tumor necrosis factor α	2.2 ± 0.6*	4.6 ± 0.9*	**	ns	**	1.8 ± 0.4	1.9 ± 0.3*	*	ns	*
hsp90aa	Heat shock protein 90a	0.9 ± 0.2	3.7 ± 0.3*	*	ns	ns	2.2 ± 0.6	3.2 ± 1.0*	**	ns	*
clec	c-type lectin	1.3 ± 0.2	1.8 ± 0.2*	*	ns	ns	1.0 ± 0.1	2.0 ± 0.2	ns	ns	ns
lysg	g-type lysozyme	0.8 ± 0.1	1.2 ± 0.3	ns	ns	ns	2.6 ± 0.2*	1.1 ± 0.1	**	**	ns
cxc10	Chemokine cxc10	3.6 ± 0.3*	1.0 ± 0.0	**	**	**	1.8 ± 0.3*	1.1 ± 0.2	*	**	*
cox2	Cyclooxygenase 2	1.7 ± 0.4	5.7 ± 2.4*	**	ns	ns	1.3 ± 0.4	2.8 ± 0.2*	*	ns	ns
c3	Complement factor 3	1.2 ± 0.1	2.6 ± 0.5*	*	*	ns	2.4 ± 0.3*	2.5 ± 0.4*	**	**	ns
ifn1	Interferon type 1	1.2 ± 0.9	2.8 ± 0.5*	*	*	ns	2.0 ± 0.2*	2.0 ± 0.1	**	ns	*
ifna3	Interferon type a3	1.0 ± 0.0	4.4 ± 0.6*	**	**	*	2.0 ± 0.2	6.1 ± 1.0*	**	*	ns
mx	GTP binding protein mx	0.7 ± 0.1	4.9 ± 1.4*	*	ns	ns	5.8 ± 1.8*	3.6 ± 1.0*	**	ns	**
irf1	Interferon regulatory factor 1	1.0 ± 0.2	1.4 ± 0.4	ns	ns	ns	1.6 ± 0.1	1.5 ± 0.1	*	ns	ns
irf2	Interferon regulatory factor 2	1.1 ± 0.2	2.5 ± 0.5	ns	ns	ns	1.9 ± 0.3*	2.0 ± 0.3	*	*	ns
irf3	Interferon regulatory factor 3	1.1 ± 0.2	3.5 ± 1.1*	*	ns	ns	1.9 ± 0.0*	2.7 ± 0.3*	**	**	ns
irf4	Interferon regulatory factor 4	1.1 ± 0.4	3.2 ± 0.9	ns	ns	ns	3.4 ± 0.3*	4.4 ± 0.3*	**	ns	**
irf5	Interferon regulatory factor 5	1.2 ± 0.2	1.6 ± 0.1	ns	ns	ns	1.3 ± 0.1	2.4 ± 0.2*	**	ns	**
irf7	Interferon regulatory factor 7	1.4 ± 0.1*	2.2 ± 0.1*	**	**	ns	2.2 ± 0.2*	2.0 ± 0.1	*	**	ns
irf8	Interferon regulatory factor 8	1.2 ± 0.2	1.8 ± 0.2	ns	ns	ns	1.4 ± 0.1	1.1 ± 0.2	ns	ns	ns
irf9	Interferon regulatory factor 9	1.2 ± 0.1	2.3 ± 0.4*	*	*	ns	2.2 ± 0.5*	2.3 ± 0.5*	**	ns	*
irf10	Interferon regulatory factor 10	1.0 ± 0.2	1.5 ± 0.3	ns	ns	ns	6.1 ± 1.7*	1.7 ± 0.2*	**	ns	**
cd4	cluster of differentiation 4	1.2 ± 0.4	2.4 ± 0.5	ns	ns	ns	3.1 ± 0.8*	3.7 ± 0.4*	**	*	ns
cd8a	cluster of differentiation 8a	0.8 ± 0.2	1.2 ± 0.5	ns	ns	*	4.0 ± 1.0*	2.1 ± 0.2	**	*	ns

Acknowledgements

This study has been funded by MCIU/AEI/FEDER, UE Project RTA2017-00054-C03-01 and cofunded 80% by Programa Operativo FEDER de Andalucía 2014–2020, project PP.AVA.AVA201601.9 "Nuevas herramientas genómicas para el análisis genético y evaluación transcriptómica de compuestos funcionales basados en microalgas para impulsar la acuicultura del lenguado (SOLEALGAE)". In addition, it was also partially supported by Proyecto de Excelencia, Junta de Andalucía, P12-RNM-2261. Carlos Carballo was supported by an INIA PhD grant (2014).

Appendix A. Supplementary data

Supplementary data related to this article can be found at https://doi.org/10.1016/j.fsi.2019.04.049.

Conflicts of interest

Authors declare there is not conflict of interests.

References

[1] J.J. Borrego, E.J. Valverde, A.M. Labella, D. Castro, Lymphocystis disease virus: its importance in aquaculture, Rev. Aquacult. 9 (2017) 179–193.
[2] D.A. Smail, A.L.S. Munro, The virology of teleosts, in: R.J. Roberts (Ed.), Fish Pathology, W.B. Saunders, Edinburgh, 2001, pp. 169–253.
[3] A. Colorni, F. Padrós, Diseases and health management, in: M. Pavlidis, C. Mylonas (Eds.), Sparidae: Biology and Aquaculture of Gilthead Sea Bream and Other Species, Wiley-Blackwell, Oxford, 2011, pp. 321–357.
[4] M. Hossain, S.R. Kim, S.I. Kitamura, D.W. Kim, S.J. Jung, T. Nishizawa, M. Yoshimizu, M.J. Oh, Lymphocystis disease virus persists in the epidermal tissues of olive flounder, Paralichthys olivaceus (Temminch & Schlegel), at low temperatures, J. Fish Dis. 32 (8) (2009) 699–703.
[5] M.C. Alonso, I. Cano, E. Garcia-Rosado, D. Castro, J. Lamas, J.L. Barja, J.J. Borrego, S.M. Bergmann, Isolation of lymphocystis disease virus from sole, *Solea senegalensis* Kaup, and blackspot sea bream, *Pagellus bogaraveo* (Brunnich), J. Fish Dis. 28 (4) (2005) 221–228.
[6] I. Cano, E.J. Valverde, B. Lopez-Jimena, M.C. Alonso, E. Garcia-Rosado, C. Sarasquete, J.J. Borrego, D. Castro, A new genotype of Lymphocystivirus isolated from cultured gilthead seabream, *Sparus aurata* L., and Senegalese sole, *Solea senegalensis* (Kaup), J. Fish Dis. 33 (2010) 695–700.
[7] I. Cano, E.J. Valverde, E. Garcia-Rosado, M.C. Alonso, B. Lopez-Jimena, J.B. Ortiz-Delgado, J.J. Borrego, C. Sarasquete, D. Castro, Transmission of lymphocystis disease virus to cultured gilthead seabream, *Sparus aurata* L., larvae, J. Fish Dis. 36 (6) (2013) 569–576.
[8] I. Cano, B. Lopez-Jimena, E. Garcia-Rosado, J.B. Ortiz-Delgado, M.C. Alonso, J.J. Borrego, C. Sarasquete, D. Castro, Detection and persistence of lymphocystis disease virus in Artemia sp, Aquaculture 291 (2009) 230–236.
[9] C. Carballo, D. Castro, J.J. Borrego, M. Manchado, Gene expression profiles associated with lymphocystis disease virus (LCDV) in experimentally infected Senegalese sole (Solea senegalensis), Fish Shellfish Immunol. 66 (2017) 129–139.
[10] H. Benzekri, P. Armesto, X. Cousin, M. Rovira, D. Crespo, M.A. Merlo, D. Mazurais, R. Bautista, D. Guerrero-Fernandez, N. Fernandez-Pozo, M. Ponce, C. Infante, J.L. Zambonino, S. Nidelet, M. Gut, L. Rebordinos, J.V. Planas, M.L. Begout, M.G. Claros, M. Manchado, De novo assembly, characterization and functional annotation of Senegalese sole (*Solea senegalensis*) and common sole (*Solea solea*) transcriptomes: integration in a database and design of a microarray, BMC Genomics 15 (2014) 952.
[11] M. Ponce, E. Salas-Leiton, A. Garcia-Cegarra, A. Boglino, O. Coste, C. Infante, E. Gisbert, L. Rebordinos, M. Manchado, Genomic characterization, phylogeny and gene regulation of g-type lysozyme in sole (*Solea senegalensis*), Fish Shellfish Immunol. 31 (6) (2011) 925–937.
[12] E. Salas-Leiton, O. Coste, E. Asensio, C. Infante, J.P. Cañavate, M. Manchado, Dexamethasone modulates expression of genes involved in the innate immune system, growth and stress and increases susceptibility to bacterial disease in Senegalese sole (*Solea senegalensis* Kaup, 1858), Fish Shellfish Immunol. 32 (5) (2012) 769–778.
[13] S. Ferraresso, A. Bonaldo, L. Parma, F. Buonocore, G. Scapigliati, P.P. Gatta, L. Bargelloni, Ontogenetic onset of immune-relevant genes in the common sole (*Solea solea*), Fish Shellfish Immunol. 57 (2016) 278–292.
[14] E. De Swaef, K. Demeestere, N. Boon, W. Van den Broeck, F. Haesebrouck, A. Decostere, Development of a reliable experimental set-up for Dover sole larvae *Solea solea* L. and exploring the possibility of implementing this housing system in a gnotobiotic model, Res. Vet. Sci. 115 (2017) 418–424.
[15] E. De Swaef, M. Vercauteren, L. Duchateau, F. Haesebrouck, A. Decostere, Experimental infection model for vibriosis in Dover sole (*Solea solea*) larvae as an aid in studying its pathogenesis and alternative treatments, Vet. Res. 49 (1) (2018) 24.
[16] E.J. Valverde, I. Cano, A. Labella, J.J. Borrego, D. Castro, Application of a new real-time polymerase chain reaction assay for surveillance studies of lymphocystis disease virus in farmed gilthead seabream, BMC Vet. Res. 12 (2016) 71.
[17] J. Roman-Padilla, A. Rodriguez-Rua, M. Manchado, I. Hachero-Cruzado, Molecular characterization and developmental expression patterns of apolipoprotein A-I in Senegalese sole (Solea senegalensis Kaup), Gene Expr. Patterns 21 (1) (2016) 7–18.
[18] J. Roman-Padilla, A. Rodriguez-Rua, M.G. Claros, I. Hachero-Cruzado, M. Manchado, Genomic characterization and expression analysis of four apolipoprotein A-IV paralogs in Senegalese sole (Solea senegalensis Kaup), Comp. Biochem. Physiol. B Biochem. Mol. Biol. 191 (2016) 84–98.
[19] J. Ortiz-Delgado, D. Simes, P. Gavaia, C. Sarasquete, M. Cancela, Osteocalcin and matrix GLA protein in developing teleost teeth: identification of sites of mRNA and protein accumulation at single cell resolution, Histochem. Cell Biol. 124 (2005) 123–130.
[20] J. Ortiz-Delgado, I. Fernández, C. Sarasquete, E. Gisbert, Normal and histopathological organization of opercular bone and vertebrae in gilthead seabream Sparus aurata, Aquat. Biol. 21 (2014) 67–84.
[21] I. Cano, P. Ferro, M.C. Alonso, C. Sarasquete, E. Garcia-Rosado, J.J. Borrego, D. Castro, Application of in situ detection techniques to determine the systemic condition of lymphocystis disease virus infection in cultured gilt-head seabream, *Sparus aurata* L, J. Fish Dis. 32 (2) (2009) 143–150.
[22] M.C. Alonso, I. Cano, D. Castro, S.I. Perez-Prieto, J.J. Borrego, Development of an in situ hybridisation procedure for the detection of sole aquabirnavirus in infected fish cell cultures, J. Virol. Methods 116 (2004) 133–138.
[23] E.J. Valverde, J.J. Borrego, D. Castro, Evaluation of an integrated cell culture RT-PCR assay to detect and quantify infectious lymphocystis disease virus, J. Virol. Methods 238 (2016) 62–65.
[24] C. Infante, M.P. Matsuoka, E. Asensio, J.P. Cañavate, M. Reith, M. Manchado, Selection of housekeeping genes for gene expression studies in larvae from flatfish using real-time PCR, BMC Mol. Biol. 9 (2008) 28.
[25] C. Carballo, E.G. Chronopoulou, S. Letsiou, C. Maya, N.E. Labrou, C. Infante, D.M. Power, M. Manchado, Antioxidant capacity and immunomodulatory effects of a chrysolaminarin-enriched extract in Senegalese sole, Fish Shellfish Immunol. 82 (2018) 1–8.
[26] M. Manchado, E. Salas-Leiton, C. Infante, M. Ponce, E. Asensio, A. Crespo, E. Zuasti, J.P. Cañavate, Molecular characterization, gene expression and transcriptional regulation of cytosolic HSP90 genes in the flatfish Senegalese sole (*Solea senegalensis* Kaup), Gene 416 (1–2) (2008) 77–84.
[27] A. Fernandez-Trujillo, P. Ferro, E. Garcia-Rosado, C. Infante, M.C. Alonso, J. Bejar, J.J. Borrego, M. Manchado, Poly I:C induces Mx transcription and promotes an antiviral state against sole aquabirnavirus in the flatfish Senegalese sole (*Solea senegalensis* Kaup), Fish Shellfish Immunol. 24 (3) (2008) 279–285.
[28] P. Armesto, M.A. Campinho, A. Rodriguez-Rua, X. Cousin, D.M. Power, M. Manchado, C. Infante, Molecular characterization and transcriptional regulation of the Na +/K+ ATPase alpha subunit isoforms during development and salinity challenge in a teleost fish, the Senegalese sole (Solea senegalensis), Comp. Biochem. Physiol. B Biochem. Mol. Biol. 175 (2014) 23–38.
[29] G. Caraux, S. Pinloche, PermutMatrix: a graphical environment to arrange gene expression profiles in optimal linear order, Bioinformatics 21 (7) (2005) 1280–1281.
[30] C. Sarasquete, M. Gonzalez-Canales, J. Arellano, S. Perez-Prieto, E. Garcia-Rosado, J.J. Borrego, Histochemical study of lymphocystis disease in skin of gilthead seabream, *Sparus aurata* L, Histol. Histopathol. 13 (1998) 37–45.
[31] G. Zimmer, G. Reuter, R. Schauer, Use of influenza C virus for detection of 9-O-acetylated sialic acids on immobilized glycoconjugates by esterase activity, Eur. J. Biochem. 204 (1) (1992) 209–215.
[32] M. van der Marel, N. Caspari, H. Neuhaus, W. Meyer, M.L. Enss, D. Steinhagen, Changes in skin mucus of common carp, Cyprinus carpio L., after exposure to water with a high bacterial load, J. Fish Dis. 33 (5) (2010) 431–439.
[33] L. Hanson, A. Dishon, M. Kotler, Herpesviruses that infect fish, Viruses 3 (11) (2011) 2160–2191.
[34] V.S. Raj, G. Fournier, K. Rakus, M. Ronsmans, P. Ouyang, B. Michel, C. Delforges, B. Costes, F. Farnir, B. Leroy, R. Wattiez, C. Melard, J. Mast, F. Lieffrig, A. Vanderplasschen, Skin mucus of Cyprinus carpio inhibits cyprinid herpesvirus 3 binding to epidermal cells, Vet. Res. 42 (2011) 92.
[35] M. Castro Cunha, P. Rodrigues, F. Soares, P. Makridis, J. Skjermo, M. Dinis, Development of the immune system and use of immunostimulants in Senegalese sole (Solea senegalensis), in: H. Browman, A. Skiftesvik (Eds.), The Big Fish Bang Proceedings of the 26th Annual Larval Fish Conference, Institute of Marine Research, Bergen, Norway, 2003.
[36] H. Cordero, A. Cuesta, J. Meseguer, M.A. Esteban, Characterization of the gilthead seabream (*Sparus aurata* L.) immune response under a natural lymphocystis disease virus outbreak, J. Fish Dis. 39 (12) (2016) 1467–1476.
[37] G. Hu, X. Chen, Q. Gong, Q. Liu, S. Zhang, X. Dong, Structural and expression studies of interferon regulatory factor 8 in Japanese flounder, *Paralichthys olivaceus*, Fish Shellfish Immunol. 35 (3) (2013) 1016–1024.
[38] G. Hu, X. Yin, H. Lou, J. Xia, X. Dong, J. Zhang, Q. Liu, Interferon regulatory factor 3 (IRF-3) in Japanese flounder, *Paralichthys olivaceus*: sequencing, limited tissue distribution, inducible expression and induction of fish type I interferon promoter, Dev. Comp. Immunol. 35 (2) (2011) 164–173.
[39] G. Hu, X. Yin, J. Xia, X. Dong, J. Zhang, Q. Liu, Molecular cloning and characterization of interferon regulatory factor 7 (IRF-7) in Japanese flounder, *Paralichthys olivaceus*, Fish Shellfish Immunol. 29 (6) (2010) 963–971.
[40] G.B. Hu, H.M. Lou, X.Z. Dong, Q.M. Liu, S.C. Zhang, Characteristics of the interferon regulatory factor 5 (IRF5) and its expression in response to LCDV and poly I:C challenges in Japanese flounder, *Paralichthys olivaceus*, Dev. Comp. Immunol. 38 (2)

(2012) 377–382.
[41] G.B. Hu, M.Y. Zhao, J.Y. Lin, Q.M. Liu, S.C. Zhang, Molecular cloning and characterization of interferon regulatory factor 9 (IRF9) in Japanese flounder, *Paralichthys olivaceus*, Fish Shellfish Immunol. 39 (2) (2014) 138–144.
[42] R. Wu, X. Sheng, X. Tang, J. Xing, W. Zhan, Transcriptome analysis of flounder (Paralichthys olivaceus) gill in response to lymphocystis disease virus (LCDV) infection: novel insights into fish defense mechanisms, Int. J. Mol. Sci. 19 (1) (2018).
[43] M.A. Fernandez-Trujillo, E. Garcia-Rosado, M.C. Alonso, D. Castro, M.C. Alvarez, J. Bejar, Mx1, Mx2 and Mx3 proteins from the gilthead seabream (*Sparus aurata*) show in vitro antiviral activity against RNA and DNA viruses, Mol. Immunol. 56 (4) (2013) 630–636.
[44] E. Gruys, M.J. Toussaint, T.A. Niewold, S.J. Koopmans, Acute phase reaction and acute phase proteins, J. Zhejiang Univ. - Sci. B 6 (11) (2005) 1045–1056.
[45] P. Kalinski, Regulation of immune responses by prostaglandin E2, J. Immunol. 188 (1) (2012) 21–28.
[46] R. Geller, S. Taguwa, J. Frydman, Broad action of Hsp90 as a host chaperone required for viral replication, Biochim. Biophys. Acta 1823 (3) (2012) 698–706.